decrease in the concentration of La^{3+} ion in the oxide (atomic ratio of La/Co is shown in Figure 4) as shown in curve B and were never observed for the as-deposited oxides containing no La^{3+} ion. These results indicate that La^{3+} ion in the $LaCoO_3$ precursor exists in a state similar to that in $La(NO_3)_3$.[12] Consequently, the $LaCoO_3$ precursor will be electrochemically deposited by the following two steps.

$$2Co^{2+} + 6H_2O \rightarrow Co_2O_3 \cdot 3H_2O + 6H^+ + 2e^- \quad (2)$$

$$Co_2O_3 \cdot 3H_2O + 2La(NO_3)_3 \rightarrow Co_2O_3 \cdot 2La(NO_3)_3 \cdot 3H_2O \ (LaCoO_3 \text{ precursor}) \quad (3)$$

Reaction 3 proceeds at a temperature higher than about 50 °C, because no incorporation of La^{3+} occurred at a temperature lower than 50 °C as already stated.

TG-DTG curves shown in Figure 7 quantitatively give the amount of water and NO_3^- in the $LaCoO_3$ precursors which were prepared at 0.95 V in the solutions with $[Co(CH_3COO)_2]/[La(NO_3)_3]$ = 0.02 M/2.0 M (A) and with $[Co(NO_3)_2]/[La(NO_3)_3]$ = 0.02 M/2.0 M (B). The weight loss below about 200 °C (part a) is based on the release of water in the oxides, while that in the temperature range from 250 to 500 °C (part b) is based on the release of NO_2. In the IR measurements, no absorption peaks due to NO_3^- (b in Figure 6) were observed for the sample prepared by heat treatment of the $LaCoO_3$ precursor at 500 °C, while those peaks were observed for the sample heated at 200 °C. All of the weight loss in Figure 7 was in harmony with the composition of the $LaCoO_3$ precursor in eq 3.

It should be noted that no La^{3+} ion had dissolved in the water from the $LaCoO_3$ precursor after an immersion for 30 min, as shown in Table I. This result is very different from the case of the $LaMnO_3$ precursor, where almost all the La^{3+} ion dissolved in the water from the $LaMnO_3$ precursor after immersion.[2] Probably, Co^{2+}, La^{3+}, NO_3^- and O^{2-} ions in the $LaCoO_3$ precursor will strongly combine with each other, although its structure is ambiguous because of its amorphous state.

Figure 8 shows the X-ray diffraction patterns of the oxide films heated at various temperatures, where the $LaCoO_3$ precursor was prepared at 0.95 V in the solution with $[Co(CH_3COO)_2]/[La(NO_3)_3]$ = 0.02 M/2.0 M. Only some $LaCoO_3$ perovskite diffraction peaks appeared with heat treatment at temperatures higher than about 500 °C, while no diffraction peak was observed when the temperature of the heat treatment was lower than 400 °C. It is worth noting that $LaCoO_3$ perovskite is formed by heat treatment even at temperatures as low as 500 °C (Figure 8), since a temperature higher than about 900 °C for heat treatment, in general, is necessary for the crystallization of $LaCoO_3$ perovskite using a ceramic technique. Consequently, the $LaCoO_3$ precursor with a composition of $Co_2O_3 \cdot 2La(NO_3)_3 \cdot 3H_2O$, is very suitable as a starting material in the preparation of $LaCoO_3$ perovskite. The reactions 4-6 will proceed during the heat-treatment, where

$$Co_2O_3 \cdot 2La(NO_3)_3 \cdot 3H_2O \xrightarrow{<200\ ^\circ C} Co_2O_3 \cdot 2La(NO_3)_3 + 3H_2O \quad (4)$$

$$Co_2O_3 \cdot 2La(NO_3)_3 \xrightarrow{250\text{-}500\ ^\circ C} 2LaCoO_3 + 6NO_2 + 1.5O_2 \quad (5)$$

$$LaCoO_3 \xrightarrow{>500\ ^\circ C} LaCoO_3 \text{ perovskite (crystallization)} \quad (6)$$

$LaCoO_3$, produced by eq 5, is amorphous. Figure 9 shows SEM micrographs of the $LaCoO_3$ precursor (A) prepared at 0.95 V in the solution with $[Co(CH_3COO)_2]/[La(NO_3)_3]$ = 0.02 M/2.0 M and $LaCoO_3$ perovskite (B) prepared by heat treatment at 1000 °C. The film thickness was about 1.5 μm and the grain size of the $LaCoO_3$ perovskite was in the range from 0.2 to 0.8 μm. Thus, a thin film of the $LaCoO_3$ perovskite was easily prepared by the present method, and its composition can be easily controlled by the applied potential. Therefore, the present method will be very useful for the preparation of the $LaCoO_3$ electrode in SOFC.

Registry No. $LaCoO_3$, 12016-86-3; $Co(CH_3COO)_2$, 71-48-7; $La(NO_3)_3$, 10099-59-9; $Co(NO_3)_2$, 10141-05-6; $CoSO_4$, 10124-43-3; $Co_2O_3 \cdot 2La(NO_3)_3 \cdot 3H_2O$, 138540-39-3; Co, 7440-48-4.

Contribution from the Department of Chemistry, University of Florence, Florence, Italy

Gadolinium(III) Complexes with Pyridine-Substituted Nitronyl Nitroxide Radicals

Cristiano Benelli, Andrea Caneschi, Dante Gatteschi,* and Luca Pardi

Received July 24, 1991

Two compounds of formula $Gd(hfac)_3(NIToPy) \cdot 0.5C_7H_{16}$ (I) and $Gd(hfac)_3(NITpPy)$ (II), respectively, where hfac = hexafluoroacetylacetonate, NIToPy = 2-(2-pyridyl)-4,4,5,5-tetramethyl-4,5-dihydro-1*H*-imidazolyl 3-oxide, and NITpPy = 2-(4-pyridyl)-4,4,5,5-tetramethyl-4,5-dihydro-1*H*-imidazolyl 3-oxide, have been synthesized. Compound I crystallizes in the monoclinic space group $P2_1/n$ with a = 1642.4 (4) pm, b = 1300.8 (8) pm, c = 2089.4 (4) pm, β = 109.85 (2)°, Z = 4, R = 0.0668, and R_w = 0.0711. The structure consists of isolated molecules where the nitronyl nitroxide radical acts as a bidentate ligand toward gadolinium(III) through the nitrogen atom of the pyridine ring and the oxygen atom of the N-O group. Compound II crystallizes in the monoclinic space group $P2_1/n$ with a = 1709.9 (4) pm, b = 1222.2 (6) pm, c = 1850.2 (5) pm, β = 93.01 (2)°, Z = 4, R = 0.0432, and R_w = 0.0464. In the solid state a NITpPy molecule is bound through the pyridine nitrogen to a $Gd(hfac)_3$ molecule and through the oxygen of the N-O group to gadolinium(III) of another asymmetric unit. In this way molecules are formed where two gadolinium(III) and two nitronyl nitroxide radicals are present. The magnetic properties of both the complexes were studied by measuring their magnetic susceptibilities at various temperatures in the 1.6-300 K range. The analysis of these data showed that a ferromagnetic coupling between the lanthanide ion and the radical is always present. This result is discussed on the basis of magnetic exchange through a spin polarization mechanism.

Introduction

Recently several compounds in which gadolinium(III) is bound to paramagnetic ligands have been reported. These can be either nitronyl nitroxide radicals[1-5] or copper(II) complexes,[6-9] but in every case a weak ferromagnetic coupling between gadolinium(III) and the other paramagnetic center has been observed. The model which has been suggested in order to justify the preferred parallel

(1) Benelli, C.; Caneschi, A.; Gatteschi, D.; Laugier, J.; Rey, P. *Angew. Chem., Int. Ed. Engl.* **1987**, *26*, 913.
(2) Benelli, C.; Caneschi, A.; Gatteschi, D.; Pardi, L.; Rey, P.; Shum, D. P.; Carlin, R. L. *Inorg. Chem.* **1989**, *28*, 272.
(3) Benelli, C.; Caneschi, A. Gatteschi, D.; Guillou, O.; Pardi, L.; Rey, P. *Inorg. Chim. Acta* **1989**, *160*, 1.
(4) Benelli, C.; Caneschi, A.; Fabretti, A. C.; Gatteschi, D.; Pardi, L. *Inorg. Chem.* **1990**, *29*, 4153.
(5) Benelli, C.; Caneschi, A.; Gatteschi, D.; Pardi, L.; Rey, P. *Inorg. Chem.* **1990**, *29*, 4223.
(6) Bencini, A.; Benelli, C.; Caneschi, A.; Carlin, R. L.; Dei, A.; Gatteschi, D. *J. Am. Chem. Soc.* **1985**, *107*, 8128.
(7) Bencini, A.; Benelli, C.; Caneschi, A.; Dei, A.; Gatteschi, D. *Inorg. Chem.* **1986**, *25*, 572.
(8) Carlin, R. L.; Vaziri, M.; Benelli, C.; Gatteschi, D. *Solid State Commun.* **1988**, *66*, 79.
(9) Benelli, C.; Caneschi, A.; Gatteschi, D.; Guillou, O.; Pardi, L. *Inorg. Chem.* **1990**, *29*, 1750.

0020-1669/92/1331-0741$03.00/0

Table I. Crystallographic Data for $Gd(hfac)_3NITToPy\cdot 0.5C_7H_{16}$ (I) and $Gd(hfac)_3NITpPy$ (II)

	(I)	(II)
formula	$GdC_{30.5}H_{27}O_8N_3F_{18}$	$GdC_{27}H_{19}O_8N_3F_{18}$
fw	1062.79	1012.68
cryst sys	monoclinic	monoclinic
space group	$P2_1/n$	$P2_1/n$
a, pm	1642.4 (1)	1709.9 (4)
b, pm	1300.8 (1)	1222.2 (6)
c, pm	2089.4 (2)	1850.2 (5)
β, deg	109.85 (1)	93.01 (2)
V, 10^6 pm^3	4198.6	3861.3
Z	4	4
ρ_{calcd}, g cm^{-3}	1.68	1.74
μ, cm^{-1}	16.70	18.16
R^a	0.0688	0.0432
$R_w{}^b$	0.0711	0.0464

$^a R = \sum||F_o| - |F_c||/\sum|F_o|$. $^b R_w = [\sum w(|F_o| - |F_c|)^2/\sum|F_o|^2]^{1/2}$; $w = 1/(\sigma^2(F) - 0.0005F^2)$.

alignment of the spins assumes that the magnetic π^* orbital of the radical has a relatively large overlap with the empty 6s orbital of gadolinium(III), transferring there some unpaired spin density and polarizing the spins of the seven electrons in the 4f orbitals.[10]

In the attempt to elaborate strategies to design extended magnetic systems using lanthanide ions and radicals we have decided to test the NITpPy and NITToPy radicals (NITpPy = 2-(4-pyridyl)-4,4,5,5-tetramethyl-4,5-dihydro-1*H*-imidazolyl 3-oxide; NITToPy = 2-(2-pyridyl)-4,4,5,5-tetramethyl-4,5-dihydro-1*H*-imidazolyl 3-oxide), which have already been found to yield interesting extended magnetic structures with transition-metal ions.[11,12] We wish to report here the crystal structure and the magnetic properties of $Gd(hfac)_3(NITToPy)\cdot 0.5C_7H_{16}$ (I) and $Gd(hfac)_3(NITpPy)$ (II) (hfac = hexafluoroacetylacetonate).

Experimental Section

Synthesis of the Complexes. $Gd(hfac)_3\cdot 2H_2O$ was prepared according to literature methods.[13,14] The NITpPy and NITToPy ligands were prepared as described elsewhere.[15,16]

Synthesis of $Gd(hfac)_3NITToPy\cdot 0.5(n\text{-heptane})$. A 0.1 mmol amount of $Gd(hfac)_3\cdot 2H_2O$ was dissolved in 15 mL of hot *n*-heptane, and then the solution was kept at 60 °C while 5 mL of a $CHCl_3$ solution containing 0.1 mmol of NITToPy was added dropwise. Then, the resulting blue-violet solution was stored at room temperature. After approximately 10 h, light violet elongated crystals were formed. They were collected and analyzed for $Gd(hfac)_3NITToPy\cdot 0.5(n\text{-heptane})$. Anal. Calcd for $C_{30.5}H_{27}O_8N_3F_{18}Gd$: C, 34.46; H, 2.56; N, 3.95. Found: C, 34.42; H, 2.51; N, 3.94.

Synthesis of $Gd(hfac)_3NITpPy$. The NITpPy derivative was prepared with the same procedure described above. Dark blue well-shaped crystals were formed in the solution after 2 days. They were collected and satisfactorily analyzed for $Gd(hfac)_3NITpPy$. Anal. Calcd for $C_{27}H_{19}O_8N_3F_{18}Gd$: C, 32.01; H, 1.88; N, 4.25. Found: C, 32.02; h, 1.91; N, 4.11.

X-ray Data Collection. X-ray data for both $Gd(hfac)_3NITToPy\cdot 0.5(n\text{-heptane})$ (I) and $Gd(hfac)_3NITpPy$ (II) were collected by using an Enraf-Nonius CAD4 diffractometer equipped with a Mo Kα X-ray tube and a graphite monochromator. Unit cell parameters and orientation matrices for data collection were derived from least-squares refinement of 25 machine-centered reflections ($10° < \theta < 17.8°$ for I and $11.5° < \theta < 16.9°$ for II). The intensity text was performed by checking four standard reflections every 9600 s, and we did not observe any significant decay for both complexes. Data were corrected for Lorentz and polarization effects but not for absorption. More details are given in Table SI (supplementary material), of which Table I is a condensed form.

Table II. Atomic Positional Parameters ($\times 10^4$) and Isotropic Thermal Factors (Å$^2 \times 10^3$) for $Gd(hfac)_3NITToPy\cdot 0.5C_7H_{16}$[a]

	x	y	z	$U_{iso}{}^b$
Gd	4300 (1)	578 (1)	2016 (1)	49
O1	5239 (4)	−550 (6)	2776 (4)	63
O2	4034 (5)	1744 (6)	2784 (4)	62
O3	2863 (5)	810 (5)	1280 (4)	62
O4	5623 (5)	1473 (7)	2587 (4)	73
O5	3825 (4)	−1013 (5)	1437 (4)	59
O6	5185 (5)	272 (6)	1364 (4)	70
O7	4273 (6)	2091 (6)	1363 (5)	81
O8	3943 (6)	−3695 (6)	2810 (5)	82
N1	3464 (5)	−465 (7)	2666 (4)	49
N2	5098 (5)	−1544 (7)	2803 (4)	54 (2)
N3	4504 (6)	−3010 (7)	2846 (5)	61 (2)
C1	3623 (6)	−1456 (8)	2882 (5)	50 (3)
C2	3117 (7)	−1959 (10)	3206 (6)	65 (3)
C3	2425 (8)	−1466 (9)	3287 (6)	68 (3)
C4	2268 (8)	−467 (10)	3075 (6)	68 (3)
C5	2799 (7)	−2 (9)	2760 (6)	62 (3)
C6	4390 (7)	−1970 (9)	2831 (6)	56 (3)
C7	5773 (7)	−2278 (10)	2756 (7)	69
C8	5443 (8)	−3305 (10)	2986 (8)	82
C9	6658 (9)	−1954 (12)	3204 (8)	101 (4)
C10	5725 (9)	−2275 (12)	2017 (7)	94 (4)
C11	5800 (10)	−3499 (13)	3748 (8)	112 (5)
C12	5511 (10)	−4235 (13)	2607 (9)	116 (5)
C13	4464 (7)	2384 (9)	3191 (6)	63 (3)
C14	5318 (9)	2673 (11)	3319 (7)	85 (4)
C15	5818 (8)	2198 (10)	2995 (7)	74 (3)
C16	3992 (10)	2921 (13)	3616 (8)	90
C17	6745 (13)	2553 (18)	3159 (14)	150
C18	2368 (7)	321 (8)	782 (6)	57 (3)
C19	2472 (7)	−679 (9)	586 (6)	62 (3)
C20	3179 (7)	−1273 (8)	925 (5)	52 (3)
C21	1567 (10)	874 (12)	353 (8)	89
C22	3215 (9)	−2371 (10)	709 (7)	76
C23	5583 (8)	835 (10)	1075 (6)	71 (3)
C24	5415 (9)	1867 (11)	934 (7)	85 (4)
C25	4770 (9)	2403 (12)	1064 (7)	87 (4)
C26	6289 (14)	364 (16)	900 (10)	126
C27	4646 (19)	3533 (17)	879 (14)	173
C28	5000	0.000	5000	341 (11)
C29	5672 (34)	361 (47)	4992 (30)	444 (11)
C30	5970 (30)	−76 (35)	4662 (23)	319 (10)
C31	6867 (23)	361 (28)	4694 (18)	265 (9)
F1	3191 (7)	2754 (12)	3412 (6)	188
F2	4322 (8)	2772 (13)	4231 (5)	202
F3	4007 (10)	3924 (9)	3564 (8)	193
F4	7260 (7)	1919 (13)	3108 (11)	241
F5	6785 (9)	3217 (13)	2703 (10)	240
F6	7065 (9)	3024 (17)	3708 (9)	282
F7	1153 (7)	504 (9)	−217 (5)	179
F8	1710 (8)	1834 (8)	272 (6)	163
F9	1001 (7)	1005 (11)	674 (6)	157
F10	3337 (6)	−3030 (5)	1198 (4)	103
F11	3898 (6)	−2503 (7)	497 (5)	115
F12	2527 (6)	−2661 (7)	195 (5)	131
F13	6808 (10)	877 (11)	757 (10)	233
F14	6056 (9)	−289 (18)	465 (12)	342
F15	6776 (12)	−138 (17)	1356 (11)	306
F16	4387 (15)	4086 (9)	1181 (10)	263
F17	5184 (13)	3913 (11)	666 (14)	314
F18	4020 (21)	3581 (17)	295 (14)	407

[a] Standard deviations in the last significant digit are in parentheses. $^b U_{iso} = {}^1/_2\sum_i\sum_j U_{ij}a_i^*a_j^*a_ia_j$.

Systematic extinctions ($h0l = 2n$; $0k0 = 2n$) are only compatible with the $P2_1/n$ space group for both I and II. The positions of the gadolinium ions were located with the heavy-atom method, and the positions of the other non-hydrogen atoms were determined by successive Fourier difference syntheses. For the NITToPy derivative the analysis of the diffraction data revealed the presence of a half-*n*-heptane molecule for each asymmetric unit with the central carbon atom occupying a special position. Its structural parameters were refined using a site occupation factor of 0.5.

For both the complexes the hydrogen atoms were introduced in the last step of the refinement procedure in calculated positions. The final

(10) Benelli, C.; Caneschi, A.; Gatteschi, D.; Pardi, L.; Rey, P. *Inorg. Chem.* **1989**, *28*, 3230.
(11) Caneschi, A.; Ferraro, F.; Gatteschi, D.; Rey, P.; Sessoli, R. *Inorg. Chem.* **1990**, *29*, 4217.
(12) Caneschi, A.; Gatteschi, D.; Sessoli, R.; Rey, P. *Inorg. Chim. Acta* **1991**, *184*, 67.
(13) Richardson, M. F.; Wagner, D. F.; Sands, D. E. *J. Inorg. Nucl. Chem.* **1968**, *30*, 1275.
(14) Lamchen, M.; Wittay, T. W. *J. Chem. Soc. C* **1966**, 2300.
(15) Ullmann, E. F.; Call, L.; Osiecki, J. H. *J. Org. Chem.* **1970**, *35*, 3623.
(16) Davis, M. S.; Morokum, K.; Kreilick, R. N. *J. Am. Chem. Soc.* **1972**, *94*, 5588.

Table III. Selected Bond Distances (Å) and Angles (deg) for $Gd(hfac)_3NITToPy\cdot 0.5C_7H_{16}$[a]

		Bonds	
Gd–O1	2.3215 (69)	Gd–O2	2.3530 (83)
Gd–O3	2.3585 (65)	Gd–O4	2.3962 (74)
Gd–O5	2.3905 (67)	Gd–O6	2.3407 (98)
Gd–O7	2.3868 (90)	Gd–N1	2.6135 (94)
O1–N2	1.3185 (79)	O2–C13	1.2278 (69)
O3–C18	1.2537 (65)	O4–C15	1.2388 (84)
O5–C20	1.2709 (64)	O6–C23	1.2630 (91)
O7–C25	1.251 (11)	O8–N3	1.2658 (88)
		Angles	
O7–Gd–N1	144.5 (3)	O6–Gd–N1	138.9 (3)
O6–Gd–O7	72.6 (3)	O5–Gd–N1	71.0 (3)
O5–Gd–O7	119.0 (3)	O5–Gd–O6	73.6 (3)
O4–Gd–N1	122.8 (3)	O4–Gd–O7	73.8 (3)
O4–Gd–O6	74.6 (3)	O4–Gd–O5	139.2 (3)
O3–Gd–N1	79.60	O3–Gd–O7	72.6 (3)
O3–Gd–O6	108.9 (3)	O3–Gd–O5	72.43
O3–Gd–O4	143.2 (3)	O2–Gd–N1	74.3 (3)
O2–Gd–O7	83.5 (3)	O2–Gd–O6	143.3 (3)
O2–Gd–O5	143.0 (3)	O2–Gd–O4	72.2 (3)
O2–Gd–O3	89.2 (3)	O1–Gd–N1	70.2 (3)
O1–Gd–O7	142.3 (3)	O1–Gd–O6	83.7 (3)
O1–Gd–O5	80.0 (2)	O1–Gd–O4	71.74
O1–Gd–O3	144.3 (3)	O1–Gd–O2	100.1 (3)
Gd–O1–N2	124.3 (5)	Gd–O2–C13	135.5 (5)
Gd–O3–C18	134.4 (5)	Gd–O4–C15	133.7 (6)
Gd–O5–C20	133.8 (4)	Gd–O6–C23	134.8 (5)
Gd–O7–C25	131.7 (6)	Gd–N1–C5	116.6 (5)
Gd–N1–C1	126.1 (5)		

[a] Standard deviations in the last significant digit are in parentheses.

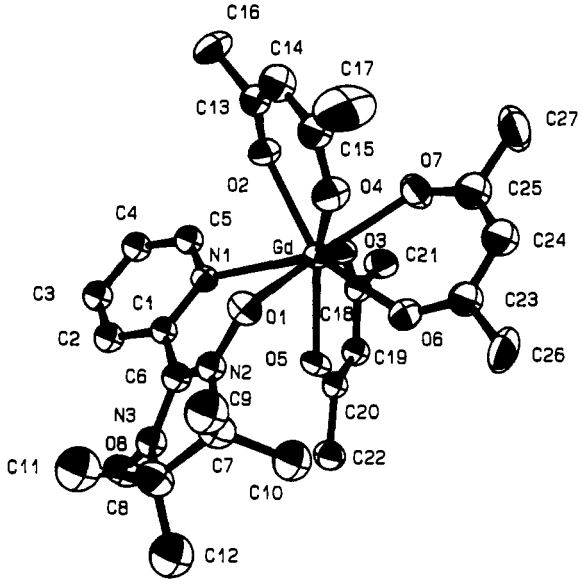

Figure 1. ORTEP drawing of the asymmetric unit of $Gd(hfac)_3NITToPy\cdot 0.5C_7H_6$. Fluorine atoms are omitted for the sake of clarity.

cycle of the least-squares refinement gave an agreement factor R of 0.0688 for I, and the highest peak in the last Fourier difference synthesis, located close to the metal atom, was about 0.6 e/Å^3. For II the final agreement factor is $R = 0.0432$ with the highest residual peak at 0.8 e/Å^3. Atomic positional parameters are listed in Table II for $Gd(hfac)_3NITToPy\cdot 0.5$(*n*-heptane) and in Table III for $Gd(hfac)_3NITpPy$. The programs used for crystallographic computation are reported in ref 17.

Magnetic Measurements. The magnetic susceptibilities for both the complexes were measured in the high-temperature range (5–300 K) with a fully automated Aztec DSM5 susceptometer equipped with an Oxford Instrument CF1200S continuous-flow cryostat and a Bruker B-E15 electromagnet operating at 1.5 T. Diamagnetic corrections were estimated from Pascal's constants. In the range 1.5–10 K range an AC mutual inductance bridge equipped with an ATNE bridge was used.

(17) (a) Sheldrick, G. SHELX76 System of Computing Programs. University of Cambridge, England, 1976. (b) Johnson, C. K. ORTEP. Report ORNL 3794; Oak Ridge National Laboratory: Oak Ridge, TN, 1965. (c) Atomic scattering factors: Cramer, D. T.; Lieberman, D. J. *J. Chem. Phys.* **1970**, *53*, 1891.

Table IV. Atomic Positional Parameters (×10^4) and Isotropic Thermal Factors (Å^2 × 10^3) for $Gd(hfac)_3NITpPy$[a]

	x	y	z	U_{iso}[b]
Gd	3014 (1)	1614 (1)	110 (1)	51
O1	2684 (3)	−220 (4)	406 (3)	64
O2	7165 (3)	3471 (5)	825 (4)	94
O3	3200 (3)	559 (4)	−950 (3)	59
O4	1886 (3)	1809 (4)	−661 (3)	67
O5	3399 (3)	2820 (4)	−821 (3)	68
O6	1969 (3)	1864 (4)	878 (3)	66
O7	3489 (3)	1183 (4)	1299 (3)	64
O8	3239 (3)	3362 (5)	601 (3)	68
N1	4539 (3)	1600 (5)	132 (3)	57
N2	2482 (3)	−1115 (5)	69 (3)	56
N3	7440 (3)	2662 (5)	513 (4)	69
C1	4947 (4)	2047 (6)	701 (4)	62 (2)
C2	5741 (4)	2149 (6)	744 (4)	55 (2)
C3	6172 (4)	1734 (6)	183 (3)	50 (2)
C4	5756 (4)	1283 (6)	−407 (4)	56 (2)
C5	4954 (4)	1238 (6)	−411 (4)	60 (2)
C6	7015 (4)	1821 (6)	211 (4)	54 (2)
C7	1667 (4)	−1559 (7)	75 (4)	68 (2)
C8	1697 (5)	−2438 (7)	−520 (5)	72 (2)
C9	1069 (5)	−645 (8)	−61 (6)	97
C10	1597 (5)	−1995 (9)	844 (5)	95
C11	1265 (5)	−3500 (8)	−370 (7)	121
C12	1471 (5)	−2027 (9)	−1268 (5)	97
C13	2902 (4)	649 (6)	−1587 (4)	60 (2)
C14	2229 (4)	1187 (7)	−1814 (4)	66 (2)
C15	1748 (4)	1691 (7)	−1331 (4)	64 (2)
C16	3372 (6)	69 (10)	−2144 (5)	90
C17	954 (6)	2106 (10)	−1600 (6)	90
C18	1880 (5)	1727 (7)	1540 (4)	70 (2)
C19	2430 (5)	1351 (7)	2058 (5)	80 (2)
C20	3185 (5)	1124 (7)	1905 (4)	66 (2)
C21	1048 (6)	1924 (12)	1775 (7)	107
C22	3740 (7)	700 (14)	2503 (6)	122
C23	3699 (4)	3747 (7)	−844 (4)	65 (2)
C24	3827 (5)	4460 (8)	−280 (5)	76 (2)
C25	3559 (4)	4237 (7)	389 (4)	65 (2)
C26	3955 (7)	4056 (10)	−1602 (6)	96
C27	3613 (8)	5115 (9)	978 (6)	100
F1	4096 (3)	197 (10)	−2056 (4)	200
F2	3150 (4)	278 (5)	−2817 (3)	115
F3	3238 (5)	−1010 (6)	−2090 (4)	140
F4	840 (3)	2128 (6)	−2305 (3)	126
F5	397 (3)	1610 (10)	−1332 (5)	207
F6	860 (5)	3130 (7)	−1428 (5)	171
F7	733 (4)	2754 (8)	1449 (5)	173
F8	608 (4)	1093 (9)	1623 (6)	220
F9	1009 (4)	2141 (8)	2450 (4)	173
F10	4135 (5)	−140 (8)	2306 (4)	180
F11	3489 (4)	571 (9)	3103 (3)	194
F12	4333 (6)	1389 (11)	2602 (5)	229
F13	4478 (4)	3390 (6)	−1815 (3)	135
F14	4235 (5)	5038 (6)	−1637 (4)	162
F15	3362 (5)	3995 (8)	−2069 (4)	165
F16	3868 (5)	4753 (6)	1589 (4)	160
F17	4061 (6)	5941 (5)	815 (4)	165
F18	2926 (5)	5547 (7)	1061 (5)	180

[a] Standard deviations in the last significant digit are in parentheses. [b] $U_{iso} = {}^1/_3\sum_i\sum_j U_{ij}a_i^*a_j^*a_ia_j$.

Results

Crystal Structures. The asymmetric units of I is shown in Figure 1. Selected bond distances and angles are reported in Table IV. The crystal structure consists of isolated molecules in which a NITToPy radical acts as a bidentate ligand toward the gadolinium ion with the oxygen atom of a N–O group and the nitrogen atom of the pyridine ring. The bite angle of the NITpPY radical acting as a bidentate ligand (O2–Gd–N1) is 70.2 (3)°. The eight coordination around the metal ion is completed by the six oxygen

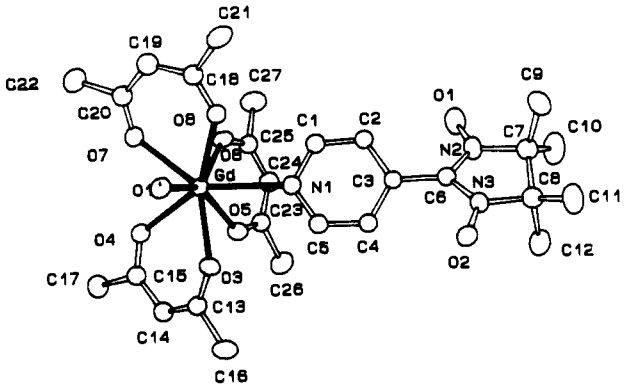

Figure 2. ORTEP drawing of the asymmetric unit of $Gd(hfac)_3NITpPy$. Fluorine atoms are omitted for the sake of clarity.

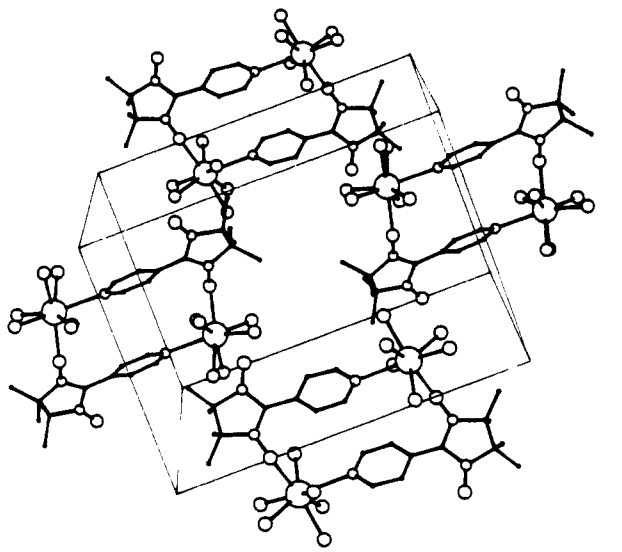

Figure 3. Schematic view of the $[Gd(hfac)_3NITpPy]_2$ unit. Fluorine atoms are omitted for the sake of clarity.

atoms of the three hfac molecules. The coordination geometry is highly distorted, and the least-squares procedures to fit it to any idealized polyhedron did not give good results.[18] All the Gd–O distances compare well with those observed either in other $Gd(hfac)_3NITR$ complexes (R = Ph, Et, *i*-Pr)[1-5] and in other reported tris(β-diketonate) eight-coordinate lanthanide complexes.[19,20] The Gd–N distance of 261.4 pm is comparable with those observed in other lanthanide–pyridine complexes (264.9 pm).[21] The pyridine ring of the radical does not deviate significantly from planarity and forms an angle of 24.60 (6)° with the O1N2C6N3O8 plane.

The shortest intermolecular contact involving atoms of the NITpPy radical is 775.7 (8) pm between the O8 atom and the N3′ atom in the molecule in the cell reported by the screw axis, and the planes of the two pyridine rings form an angle of 38.17 (2)° with distances ranging from 446 (1) to 928 (3) pm. Statistical disorder simulates a pseudosymmetry of the *n*-heptane molecule contained in the unit cell, whose central C28 carbon atom is on an inversion center.

The asymmetric unit of $Gd(hfac)_3NITpPy$ consists of $Gd(hfac)_3$ moiety with one NITpPy molecule bonded through the oxygen atom of the N–O group and another one through the nitrogen atom of the pyridine ring as shown in Figure 2. At the same time a nitronyl nitroxide molecule, which binds a gadolinium ion with the oxygen atom of the N–O group, is coordinated through the nitrogen atom of the pyridine ring to the gadolinium ion related to the inversion center, in such a way that dimeric units $[Gd(hfac)_3NITpPy]_2$ are formed as shown in Figure 3. Relevant bond distances and angles are listed in Table V. Even in this case it is not possible to approximate the coordination geometry around the metal ion to any idealized polyhedron.[18] The Gd–O and Gd–N bond distances compare well with those reported in the literature for the same type of bonds.[19-21]

In the $Gd_2(hfac)_6(NITpPy)_2$ cluster the two pyridine rings interact in a π fashion. In fact the two units forming the cluster are reported by the inversion center, and therefore, the two rings, which do not deviate substantially from planarity, are parallel to each other. The shortest contact between atoms of the two rings in the dimeric unit is 339 (1) pm between C4 and C4′, while the Gd–Gd intramolecular distance is 788 (2) pm.

Magnetic Properties. The χT vs T plot for I is shown in Figure 4 in the 4.2–300 K range. The observed room-temperature χT value (8.06 emu mol^{-1} K) compares quite well with the value expected for noninteracting gadolinium(III) ($S_1 = {}^7/_2$) and organic radical ($S_2 = {}^1/_2$)[22] (8.10 emu mol^{-1} K). On decrease of the

Table V. Selected Bond Distances (Å) and Angles (deg) for $Gd(hfac)_3NITpPy$[a]

Bonds			
Gd–O1	2.383 (5)	Gd–O3	2.383 (5)
Gd–O4	2.349 (5)	Gd–O5	2.386 (5)
Gd–O6	2.360 (5)	Gd–O7	2.364 (5)
Gd–O8	2.344 (6)	Gd–N1	2.607 (6)
O1–N2	1.297 (8)	O2–N3	1.249 (9)
O3–C13	1.262 (9)	O4–C15	1.258 (9)
O5–C23	1.245 (10)	O6–C18	1.253 (10)
O7–C20	1.262 (10)	O8–C25	1.272 (10)
N1–C1	1.348 (10)	N1–C5	1.334 (10)
N2–C7	1.495 (10)	N1–C6	1.361 (10)
Angles			
O8–Gd–N1	81.8 (2)	O7–Gd–N1	71.9 (2)
O7–Gd–O8	78.5 (2)	O6–Gd–N1	141.2 (2)
O6–Gd–O8	76.3 (2)	O6–Gd–O7	72.7 (2)
O5–Gd–N1	72.6 (2)	O5–Gd–O8	70.8 (2)
O5–Gd–O7	135.6 (2)	O5–Gd–O6	127.0 (2)
O4–Gd–N1	143.0 (2)	O4–Gd–O8	104.8 (2)
O4–Gd–O7	145.0 (2)	O4–Gd–O6	74.3 (2)
O4–Gd–O5	75.4 (2)	O3–Gd–N1	80.4 (2)
O3–Gd–O8	141.8 (2)	O3–Gd–O7	126.2 (2)
O3–Gd–O6	134.7 (2)	O3–Gd–O5	71.7 (2)
O3–Gd–O4	72.3 (2)	O1–Gd–N1	103.8 (2)
O1–Gd–O8	143.5 (2)	O1–Gd–O7	69.5 (2)
O1–Gd–O6	77.7 (2)	O1–Gd–O5	145.6 (2)
O1–Gd–O4	92.2 (2)	O1–Gd–O3	74.0 (2)
Gd–O1–N2	138.0 (4)	Gd–O3–C13	131.0 (5)
Gd–O4–C15	133.8 (5)	Gd–O5–C23	135.8 (5)
Gd–O6–C18	135.0 (5)	Gd–O7–C20	134.5 (5)
Gd–O8–C25	135.3 (5)	Gd–N1–C5	124.1 (4)
Gd–N1–C1	119.0 (4)		

[a] Standard deviations in the last significant digit are in parentheses.

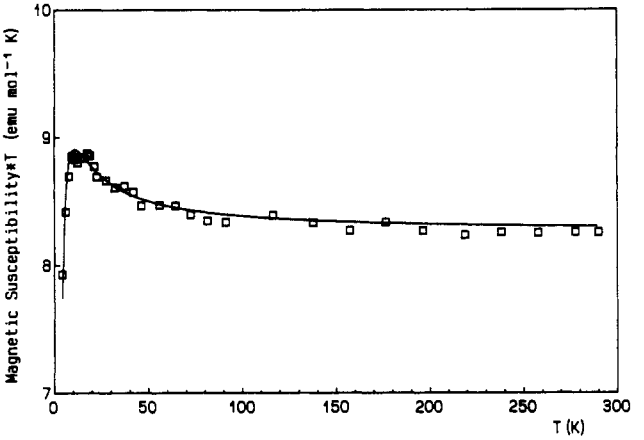

Figure 4. Temperature dependence of χT in the 4.2–300 K range for $Gd(hfac)_3NITpPy{\cdot}0.5C_7H_6$. The curve represents the fit to the experimental data (open squares) with the model described in the text.

(18) Dollase, W. A. *Acta Crystallogr., Sect. A* **1974**, *30*, 513.
(19) Drew, M. G. B. *Coord. Chem. Rev.* **1977**, *24*, 179.
(20) Sinha, S. P. *Struct. Bonding (Berlin)* **1976**, *25*, 69.
(21) Cramer, R. E.; Seff, K. *Acta Crystallogr., Sect. B* **1972**, *28*, 3281.

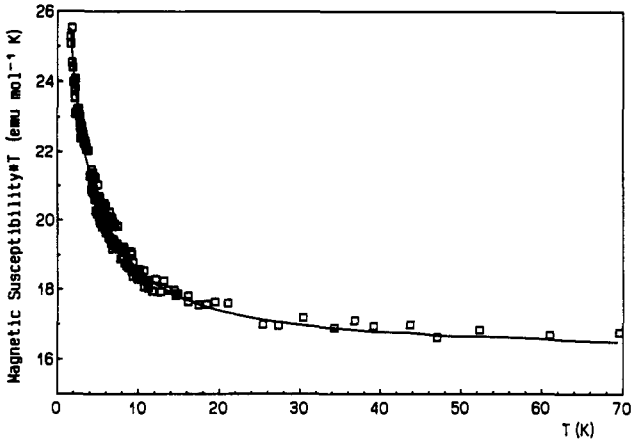

Figure 5. Temperature dependence of χT in the 1.6–70 K range for $Gd(hfac)_3NITpPy$. The curve represents the fit to the experimental data (open squares) with the model described in the text.

temperature, a steady increase in the χT values is observed with a maximum at about 9.5 K. Below this temperature χT decreases to 7.83 emu mol^{-1} K at 4.2 K. As the crystal structure showed that in the solid state there are isolated molecules containing one gadolinium and one nitronyl nitroxide, the magnetic behavior was analyzed as due to the interaction between these two spins. By using the isotropic Hamiltonian $H = J\mathbf{S}_1\cdot\mathbf{S}_2$, the usual van Vleck's equation for this type of dimer, modified to account for the magnetic field strength,[2] was derived and used in a fitting procedure through a SIMPLEX routine[23] to yield $J = -3.03$ (5) cm^{-1} with the g values fixed at $g = 1.98$ for gadolinium and $g = 2$ for the organic radical, respectively. The satisfactory agreement between experimental and calculated values ($r = 1.1 \times 10^{-2}$)[24] in the whole range of temperature indicates that the observed decrease of χT values below 9.5 is due to saturation effects. No reasonable fit could be obtained if only the dipolar interaction between the spins is taken into account.

The χT vs T plot for II is shown in Figure 5 in the range 1.6–70 K. χT is practically constant from room temperature to about 20 K, and below it increases steadily. The high-temperature value corresponds fairly well to that expected for two $S_1 = {}^7/_2$ and two $S_2 = {}^1/_2$ spins (16.18 emu mol^{-1} K is the expected value calculated for a dimeric $[Gd(hfac)_3NITpPy]_2$ unit, and 16.09 emu mol^{-1} K, the observed one). The χT value observed at the lowest temperature (1.62 K) is 25.27 emu mol^{-1} K.

The simplest model to analyze the magnetic behavior of the NITpPY derivative is to consider that a magnetic interaction is operative only through the N–O group of the radical directly bonded to the gadolinium ion. In this case the magnetic susceptibility of the dimeric $[Gd(hfac)_3NITpPy]_2$ observed in the crystal structure should be the sum of the susceptibility of two Gd–radical pairs. If a ferromagnetic interaction is assumed as observed in the NIToPy derivative, the upper limit of χT is 20 emu mol^{-1} K. As the observed value of χT at the lowest temperature we were able to reach is definitely higher than this limit, it is necessary to consider that some other exchange interaction is operative in the system.

As in similar compounds formed by the NITpPy radical with 3d metal ions a significant magnetic interaction was observed through the nitrogen atom of the pyridine ring,[12,13] we introduce an additional coupling constant, J_2, relative to the gadolinium–pyridine interaction in addition to J_1 relative to the Gd–O–N interaction. In this assumption the magnetic behavior of the system can be analyzed on the basis of that expected for a ring of four alternating spins as shown in Scheme I.[25]

Scheme I

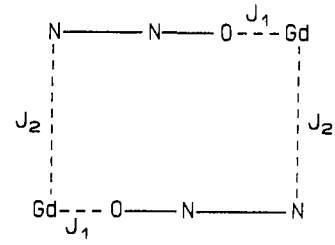

Table VI. Coupling Constants[a] in Gadolinium Nitronyl–Nitroxide Coupled Species

complex	J_{Gd-r}	J_{r-r}	ref
1:1 Species			
$[Gd(hfac)_3(NITiPr)(H_2O)]$[b]	−0.60		7
$[Gd(hfac)_3(NIToPy)]$[c]	−3.03		this work
$[Gd(hfac)_3(NITpPy)]$[d] (J)	−1.78		this work
$[Gd(hfac)_3(NITpPy)]$[d] (J')	−0.17		this work
1:2 Species			
$[Gd(hfac)_3(NITPh)_2]$[e]	−1.23	5.1	8
$[Gd(hfac)_3(NITEt)_2]$[f]	−0.50	4.3	9

[a] cm^{-1}. [b] NITiPr = 2-isopropyl-4,4,5,5-tetramethyl-4,5-dihydro-1*H*-imidazolyl-1-oxyl 3-oxide. [c] NIToPy = 2-(2-pyridyl)-4,4,5,5-tetramethyl-4,5-dihydro-1*H*-imidazolyl 3-oxide. [d] NITpPy = 2-(4-pyridyl)-4,4,5,5-tetramethyl-4,5-dihydro-1*H*-imidazolyl 3-oxide. [e] NITPh = 2-phenyl-4,4,5,5-tetramethyl-4,5-dihydro-1*H*-imidazolyl-1-oxyl 3-oxide. [f] NITEt = 2-ethyl-4,4,5,5-tetramethyl-4,5-dihydro-1*H*-imidazolyl-1-oxyl 3-oxide.

If only the nearest-neighbor interactions are considered, three different ground states are possible: (i) if J_1 and J_2 are both antiferromagnetic, the ground state has $S = 6$ and the corresponding χT value is 21 emu mol^{-1} K; (ii) if J_1 and J_2 are both ferromagnetic, the ground state has $S = 8$ and the corresponding χT value is 32 emu mol^{-1} K; (iii) if J_1 and J_2 have an opposite sign, the ground state is a diamagnetic one. It is worth noting that the spin multiplicity of the ground state does not depend on the relative intensity of the two coupling contants but only on their sign.

Using a suitable Hamiltonian to account for the Gd–radical interactions, it was possible to compute the magnetic susceptibility for the four-spin system shown in Scheme I. The fitting procedure yielded as best fit parameters $J_1 = -1.78$ (2) cm^{-1} and $J_2 = -0.17$ (4) cm^{-1} ($r = 1.3 \times 10^{-2}$). Of course there is no way to experimentally assign J_1 and J_2 to the two different exchange pathways through the N–O and pyridine nitrogen. However, comparison with the J values observed in other NITR complexes collected in Table VI suggests that J_1 can be associated with the interaction through the N–O group.

The possibility of exchange interactions between the two radicals and the two gadolinium ions in the dimeric unit cannot be ruled out, at least in principle. As concerns the 4f ions, they are so far apart from each other that we decided not to take into account any interactions between them. In other Gd(III)–NITR systems we have studied, we always observed the presence of an antiferromagnetic interaction between two radicals bonded to the central atom both through the N–O group. If a term considering the radical–radical interaction (J_{rr}) is introduced in the Hamiltonian, the calculations showed that the fitting to experimental data did not improve at all and the J_1 and J_2 values have the same values as in the simple model, while $J_{rr} = 0.016$ cm^{-1}.

Conclusions. The coupling between gadolinium(III) and both NIToPy and NITpPy is ferromagnetic, in agreement with previous results with other paramagnetic ligands.[1-5] The observed variations in the coupling constants with various NITR radicals are not large, as shown by Table VI. In the comparison of the calculated J values it must be recalled that the accuracy of the determination of ferromagnetic coupling constants is low.

As far as the pyridine moieties are concerned, the evidence for NITpPy is of a weak ferromagnetic coupling, analogous to that observed in manganese(II) complexes.[11,12] Presumably a spin

(22) Carlin, R. L. *Magnetochemistry*; Springer-Verlag: New York, 1986.
(23) James, F.; Roos, M. *Comput. Phys. Commun.* **1975**, *10*, 343.
(24) r is defined as $[\sum(\chi T_{obs} - \chi T_{calc})^2/\sum(\chi T_{obs})^2]^{1/2}$.
(25) Kahn, O. In *Organic and Inorganic Low Dimensional Crystalline Materials*; Delheas, P., Drillon, M., Eds.; Plenum Press: New York, 1987; pp 93–108.

polarization mechanism must be operative also in this case. For NITOPy no safe conclusions can be reached about the relative efficiency of the pyridine and N–O exchange pathways. However, the largest J value observed for this radical may indicate a sizeable ferromagnetic coupling is transmitted through the pyridine ring.

Acknowledgment. The financial support of the CNR, of the Progetto Finalizzato "Materiali Speciali per Tecnologie Avanzate", and of MURST is gratefully acknowledged.

Registry No. I, 138606-21-0; II, 138606-22-1; $Gd(hfac)_3$, 14354-49-5.

Supplementary Material Available: Table SI, listing crystallographic and experimental parameters for I and II, and Tables SII, SIII, SV, and SVI, listing bond distances and angles and anisotropic thermal factors for I and II (15 pages); Tables SIV and SVII, listing observed and calculated structure factors for I and II (46 pages). Ordering information is given on any current masthead page.

Contribution from the Department of Chemistry, University of Auckland, Private Bag, Auckland, New Zealand

Preparation of Group 15 (Phosphorus, Antimony, and Bismuth) Complexes of *meso*-Tetra-*p*-tolylporphyrin (TTP) and X-ray Crystal Structure of $[Sb(TTP)(OCH(CH_3)_2)_2]Cl$

Tanya Barbour, Warwick J. Belcher, Penelope J. Brothers,* Clifton E. F. Rickard, and David C. Ware

Received June 11, 1991

The syntheses of cationic phosphorus(V) and antimony(V) *meso*-tetra-*p*-tolylporphyrin (TTP) complexes $[P(TTP)X_2]X$ (X = Cl, OH) and $[Sb(TTP)X_2]X'$ (X, X': Cl, $SbCl_6$; Cl, Cl; OH, OH) and the bismuth(III) complex $[Bi(TTP)]NO_3$ are described. Reactions of the phosphorus and antimony chloro complexes with alcohols and primary amines produce the new alkoxo and aryloxo complexes $[P(TTP)(OR)_2]X$ (R, X: CH_3, Cl; CH_2CH_3, Cl; $CH(CH_3)_2$, Cl; $CH_2CH(CH_3)_2$, Cl; $CH_2C(CH_3)_3$, Cl; *p*-$C_6H_4CH_3$, Cl; *p*-C_6H_4OH, OH; *o*-C_6H_4OH, OH) and $[Sb(TTP)(OR)_2]Cl$ (R = CH_3, CH_2CH_3, $CH(CH_3)_2$, $CH_2CH(CH_3)_2$), and the amido complex $[P(TTP)(NH\text{-}p\text{-}C_6H_4CH_3)_2]Cl$. ^{31}P NMR data recorded for the phosphorus porphyrin complexes reveal the marked upfield shift of the coordinated phosphorus atom, and unusual seven-bond P–H coupling in the complexes with *p*-tolyl substituents on the axial ligands. A variable-temperature ^1H NMR study of $[Bi(TTP)]NO_3$ permits observation on the NMR time scale of aryl ring rotation on the porphyrin periphery. The structure of $[Sb(TTP)(OCH(CH_3)_2)_2]Cl$ was determined by a single-crystal X-ray structure analysis. It crystallizes in the space group $P\bar{1}$ with a = 13.515 (5) Å, b = 14.628 (4) Å, c = 15.709 (3) Å, α = 109.59 (2)°, β = 94.38 (2)°, γ = 102.19 (3)°, V = 2823 (1) Å^3, and Z = 2. The structure was refined to R = 0.081 and R_w = 0.083. The Sb atom is displaced 0.030 Å from the mean porphyrin plane and the average Sb–O bond distance is 1.935 Å.

Introduction

Although the coordination of most of the metallic elements to the porphyrin macrocycle has been demonstrated, for many years it was transition-metal porphyrin complexes which were the focus of the most intense attention. More recently, there has been a resurgence of interest in main-group chemistry, driven by the search for new conducting materials and new chemotherapeutic agents and the recent discovery of previously unsuspected bonding modes for main-group elements. Porphyrin complexes of the main-group elements have not been excluded from this renewed interest, and there has been recent activity in the study of elements from groups 13 and 14 coordinated to the porphyrin macrocycle.[1]

The insertion of antimony into mesoporphyrin dimethyl ester and etioporphyrin in 1969 provided the first examples of porphyrin complexes containing a group 15 element.[2] However, both this report and a 1974 paper describing the preparation of arsenic, antimony, and bismuth octaethylporphyrin complexes[3] engendered some confusion regarding the formulation of the products and the oxidation state of the central element. A later review correctly assigns the oxidation state and cationic nature of the six-coordinate arsenic(V) and antimony(V) complexes $[E(Por)X_2]^+$ (E = As, Sb; X = halide, OH^-) and the bismuth(III) complex $[Bi(OEP)]NO_3$.[4,5] Although both this review[4] and another account[6] refer to the preparation of a number of arsenic, antimony, and bismuth tetraarylporphyrin complexes, there have been no experimental details reported in the primary literature for any porphyrin species containing these elements since the 1969 and 1974 accounts in which the products were incorrectly characterized.[2,3] However, the formulation of the antimony species has been confirmed by an X-ray crystal structure analysis of $[Sb(OEP)(OH)_2]ClO_4 \cdot CH_3CH_2OH$.[7]

In contrast to the rather poorly documented heavier group 15 element porphyrin complexes, the coordination of the lighter element phosphorus to the porphyrin macrocycle has received some attention. The insertions of phosphorus into H_2TPP[8] and H_2OEP[9] were reported by independent workers in 1977. Since then, the spectroscopic and electrochemical behavior of the $[P(Por)X_2]^+$ (X = OH^-, Cl^-) ion has been reported[10-14] along with an X-ray crystal structure determination of $[P(TPP)(OH)_2]OH \cdot 2H_2O$.[11]

The availability of two oxidation states for the elements P, As, and Sb offers the possibility of redox chemistry of the coordinated element. In fact, UV/visible spectroscopic data have been observed for reactive but poorly characterized species proposed to be phosphorus(III), arsenic(III), and antimony(III) porphyrin com-

(1) (a) Guilard, R.; Kadish, K. M. *Chem. Rev.* **1988**, *88*, 1121. (b) Guilard, R.; Lecomte, C.; Kadish, K. M. *Struct. Bonding* **1987**, *64*, 205. (c) Kadish, K. M. *Prog. Inorg. Chem.* **1986**, *34*, 435.
(2) Treibs, A. *Liebigs Ann. Chem.* **1969**, *728*, 115.
(3) Buchler, J. W.; Lay, K. L. *Inorg. Nucl. Chem. Lett.* **1974**, *10*, 297.
(4) Sayer, P.; Gouterman, M.; Connell, C. R. *Acc. Chem. Res.* **1982**, *15*, 73.
(5) Abbreviations for porphyrinato dianions: Por, unspecified; Etio, etioporphyrinato; MPDME, dianion of mesoporphyrin dimethyl ester; OEP, octaethylporphyrinato; TPP, *meso*-tetraphenylporphyrinato; TTP, *meso*-tetra-*p*-tolylporphyrinato.
(6) Buchler, J. W. In *The Porphyrins*; Dolphin, D., Ed.; Academic Press: New York, 1978; Vol. 1, Chapter 10.
(7) Fitzgerald, A; Stenkamp, R. E.; Watenpugh, K. D.; Jensen, L. H. *Acta Crystallogr.* **1977**, *B33*, 1688.
(8) Carrano, C. J.; Tsutsui, M. *J. Coord. Chem.* **1977**, *7*, 79.
(9) Sayer, P.; Gouterman, M.; Connell, C. R. *J. Am. Chem. Soc.* **1977**, *99*, 1082.
(10) Marrese, C. A.; Carrano, C. J. *J. Chem. Soc., Chem. Commun.* **1982**, 1279.
(11) Mangani, S.; Meyer, E. F.; Cullen, D. L.; Tsutsui, M.; Carrano, C. J. *Inorg. Chem.* **1983**, *22*, 400.
(12) Marrese, C. A.; Carrano, C. J. *Inorg. Chem.* **1983**, *22*, 1858.
(13) Marrese, C. A.; Carrano, C. J. *Inorg. Chem.* **1984**, *23*, 3961.
(14) Gouterman, M.; Sayer, P.; Shankland, E.; Smith, J. P. *Inorg. Chem.* **1981**, *20*, 87.

0020-1669/92/1331-0746$03.00/0